Electronic Supplementary Information

Comparative Study of Electron Transport Through Aromatic Molecules on Gold Nanoparticles: Insights from Soft X-ray Spectroscopy of Condensed Nanoparticle Films Versus Flat Monolayer Films

Shogo Tendo,[a] Akinobu Niozu,[b] Kakuto Yoshioka,[b] Masataka Tabuse,[b] Jun-ichi Adachi,[c, d] Hirokazu Tanaka,[c] and Shin-ichi Wada [*a, b, e]

[a.] *Graduate School of Science, Hiroshima University, Higashi-Hiroshima 739-8526, Japan.*

[b.] *Graduate School of Advanced Science and Engineering, Hiroshima University, Higashi-Hiroshima 739-8526, Japan.*

[c.] *Photon Factory, Institute of Materials Structure Science, High Energy Accelerator Research Organization, Tsukuba 305-0801, Japan.*

[d.] *Graduate Institute for Advanced Studies, SOKENDAI, Tsukuba 305-0801, Japan.*

[e.] *Research Institute for Synchrotron Radiation Science, Hiroshima University, Higashi-Hiroshima 739-0046, Japan.*

** Corresponding author*

Preparation of flat films with aromatic molecules

The Au substrates used for the flat films were prepared via vacuum deposition. The SAMs of aromatic thiolate were prepared using the conventional immersion method. Single-side polished Si(100) wafers (Electronics and Materials Corporation Ltd.) were cut into 10 mm^2 and coated with a 5-nm-thick layer of Ti, followed by a 100-nm-thick Au layer. The deposition was performed at a low rate of less than 1 Å/s to prevent disordered accumulation. Organic contamination on the Au surface was removed via piranha cleaning.[1,2] Without further roughness assessment, the Au substrates were immediately immersed in a 1 mM aromatic thiol solution at 25°C for 1 day, after which their surfaces were rinsed with ethanol.

Preparation of NP films coated with aromatic molecules

A 527 nm light beam, generated from a nanosecond-pulsed Nd: YLF laser (Spectra-Physics, Empower) with a power output of 9 mJ/pulse was focused through a lens (f = 200 mm) to ablate a 10-mm-diameter Au disk (Nilaco, 99.95%) immersed in ethanol solution for 6 hours (Fig. 2 (a)). The liquid surface was positioned 8 mm above the Au surface. Following the analytical method developed by Haiss et al.,[3] the number density and average particle size of the obtained AuNP colloidal solution were determined to be ~10^{10} cm^{-3} and ~7 nm, respectively, based on ultraviolet-visible (UV–Vis) spectroscopy (SHIMADZU, UV-1800) measurements (Fig. S1 (a)). The average particle sizes were further validated using scanning electron microscopy images (Fig. S1 (b)).

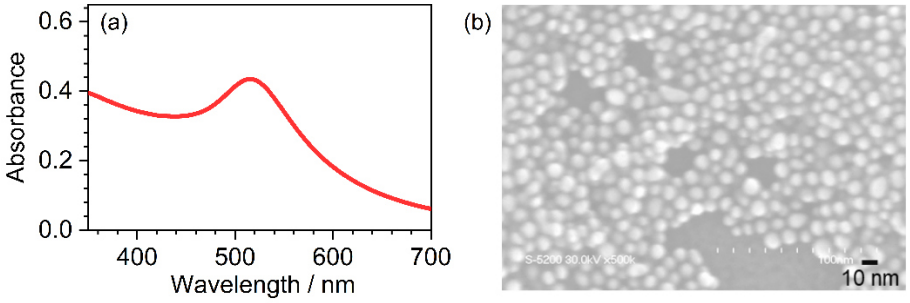

Figure S1. (a) UV–Vis absorption spectrum of AuNPs. The peak position of surface plasmon resonance was observed at 517 nm. (b) Scanning electron microscopy image of AuNPs on a Si substrate.

The AuNP colloidal solution was mixed with a 1 mM thiol solution in a 1:1 volume ratio and then stirred at 1000 rpm at 30°C for 2 days to prepare AuNPs coated with aromatic SAMs. To remove residual solute molecules, 1 mL of the solution was centrifuged (Eppendorf Centrifuge 5425) at 12,000 rpm for 90 min. The aromatic molecule-coated AuNPs were precipitated, the supernatant was removed, and the remaining precipitate was diluted in ethanol. After three rounds of centrifugation, the original solution was diluted by ~3,000 times, as confirmed via UV–Vis spectroscopy. Approximately 1 mL of the solution was dropped onto Au substrates, forming the NP films, which were subsequently dried and stored in a nitrogen atmosphere.

Experimental setup for TOF-MS measurements

For multi-bunch operation at PF, SR is a pseudo-continuous light consisting of pulses at 2 ns interval. In the hybrid operation mode, on the other hand, high current pulses (red) with 624 ns interval are included in the multi-bunch trains (blue), as shown in Fig. 2 (c). By using a pulse selector, these high-current pulses were selectively extracted every 7 pulses, and the included low-current multi-bunch components were about three orders of magnitude lower than the high-current ones. Cations desorbed by irradiation of the sample with SR pulses were mass-separated by flight time of the drift tube triggered by the pulses at this 4.368 μs interval and detected in a microchannel plate.

Overview of XPS spectra

The C 1s, S 2p, and Au 4f photoelectron spectra were measured at a photon energy of 396 eV, and the O 1s spectra were measured at a photon energy of 650 eV. In the O 1s spectra shown in Fig. 3 (a), peaks originating from the oxygen of the carbonyl group (~531.7 eV) and methoxy group (~534 eV) were observed.[4] The area ratio of the peaks was close to 1:1 for all the NP and flat films, corresponding to the number ratio of the carbonyl and ether oxygen atoms of each molecule. Three peaks were observed in the C 1s spectra (Fig. 3 (b)),[5,6] originating from the phenyl ring (~285 eV), C–S bond or methoxy (~287 eV), and carbonyl (~289 eV) carbons.

In the S 2p spectra (Fig. 3 (c)), the fitted components of the measured doublet peaks corresponded to the spin–orbit splitting of S $2p_{3/2}$ and S $2p_{1/2}$, exhibiting an energy difference of 1.2 eV and an intensity ratio of 2:1. The spectra showed two components corresponding to different chemical states: the main peaks ($2p_{3/2}$: ~162 eV) from chemisorbed (S–Au) sulfur, and the subpeaks ($2p_{3/2}$: ~163 eV) from physisorbed (S–H) sulfur or possibly sulfur in molecules damaged via soft X-ray irradiation.[7] From the fitting analysis, the proportions of physisorption for the flat films were obtained to be 35% for MP and 25% for MBP, while those for the NP films were determined to be 33% for MP and 24% for MBP. Although the films contain abundant physisorption component, the agreement of the proportions indicates that the molecules seemed to form a monolayer on the NP surfaces as well as flat surfaces. Compared with the flat films, the S 2p XPS spectra of the NP films exhibited broader peaks with spin–orbit splitting not clearly observed. This broadening might be attributed to differences in adsorption sites between the S atoms. Notably, this broadening, which is absent in molecular-coated AuNPs prepared via chemical reduction,[9,10] might be ascribed to the synthesis process.

In the Au 4f spectra (Fig. 3 (d)), two peaks for $4f_{7/2}$ (84.0 eV) and $4f_{5/2}$ (87.6 eV) were observed owing to spin–orbit splitting.[8] The NP films exhibited an increased background at higher binding energy than the flat films, attributable to the inelastic scattering of photoelectrons. This was evident in the wide-scan spectra of the high binding-energy features (Fig. S2). Moreover, peak broadening of Au 4f was observed in the NP films, probably attributable to the inherent nonuniformity of the AuNP surfaces.

Effective thickness of molecular layers

The effective thickness of aromatic molecules on the NP and flat surfaces was estimated using the peak intensities of the C 1s and Au 4f spectra (Fig. S2) by means of thickogram analysis, a graphical method to measure film thickness via XPS.[11] As shown in the figure, the relative intensities of C 1s to Au 4f differed between the NP and flat films. An HD SAM (flat monolayer film) with 17.3 Å thickness was used to determine the sensitivity factor of the thickogram.[12] Through the thickogram analysis program COMPRO12,[13] the molecular layer thicknesses of the flat films were determined to be 7.5 Å for MP and 14 Å for MBP and those of the NP films were determined to be 10 Å for MP and 19 Å for MBP. These values for the flat films were almost identical to those for SAMs of molecules with the same aromatic backbones.[14,15] The thickness of MBP was 1.9 times greater than that of MP for both NP and flat films. The chain length

dependence of thickness for the NP films matched with that for the flat films, suggesting that SAMs had identically been formed on both the NP and flat metal surfaces. The AuNPs used in this study have a particle diameter of 7 nm, which is sufficiently larger than the escape depth of photoelectrons. Molecules also adsorb on the back surfaces of the NPs, but it is considered that the photoelectrons emitted from the backs are not detected via NPs. Thus, the thickness of the molecular layers on NPs was successfully measured even under condensed condition. The molecular thicknesses of the NP films exceeded those of the flat films. This was attributed to the increased effective thickness of the molecules adsorbed on the spherical surfaces in the direction of the detector.

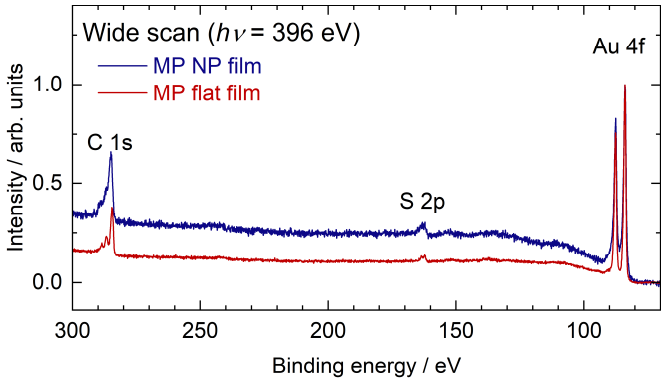

Figure S2. Wide-scan XPS spectra of flat (red line) and NP films (blue line) of MP. The photon energy was set to 396 eV and intensities of spectra were normalized at Au $4f_{7/2}$.

Molecular orientation of flat monolayers via C K-edge NEXAFS

As shown in Fig.4, the spectra of the flat monolayer films exhibited an evident polarization angle dependence, corresponding to the orientation of the molecules on the metal substrates. To derive the orientation angles of both MP and MBP molecules in the flat films, we performed a fitting analysis to the first π_1* peak with Gaussian functions and used an analytical formula for a vector-type orbital:

$$I \propto \left\{ \frac{P}{3}\left[1+(3\cos^2\theta-1)(3\cos^2\alpha-1)\right]+\frac{1-P}{2}\sin^2\gamma \right\},$$

where P denotes the incident SR light polarization, θ denotes the angle between the incident light and substrate surface, and γ denotes the angle between the surface normal and a transition dipole moment vector perpendicular to the phenyl ring, which corresponds to the tilting angle of the phenyl ring from the surface.[16] The intensities of the π_1* peak yielded γ of 67° for MP and 74° for MBP, which almost agree with those reported for aromatic SAMs with various terminal substituents.[17–19] These results revealed that the aromatic molecules were in an upright orientation relative to the substrate surface.

TIY and PIY spectra of NP films

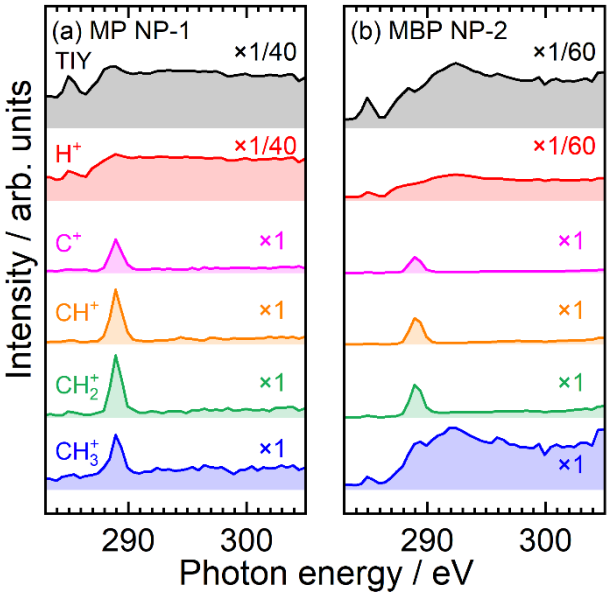

Figure S3. TIY and PIY spectra of (a) MP and (b) MBP NP films prepared from different batches. Unlike in Fig. 6, (a) shows satisfactory selectivity of MP and (b) shows poor selectivity of MBP.

Reference

1 J. B. Schlenoff, M. Li and H. Ly, Stability and Self-Exchange in Alkanethiol Monolayers, *J. Am. Chem. Soc.*, 1995, **117**, 12528–12536.

2 D. Y. Petrovykh, H. Kimura-Suda, A. Opdahl, L. J. Richter, M. J. Tarlov and L. J. Whitman, Alkanethiols on Platinum: Multicomponent Self-Assembled Monolayers, *Langmuir*, 2006, **22**, 2578–2587.

3 W. Haiss, N. T. K. Thanh, J. Aveyard and D. G. Fernig, Determination of Size and Concentration of Gold Nanoparticles from UV−Vis Spectra, *Anal. Chem.*, 2007, **79**, 4215–4221.

4 S. Wada, M. Takigawa, K. Matsushita, H. Kizaki and K. Tanaka, Adsorption and structure of methyl mercaptoacetate on Cu(111) surface by XPS and NEXAFS spectroscopy, *Surface Science*, 2007, **601**, 3833–3837.

5 C. M. Whelan, M. R. Smyth and C. J. Barnes, HREELS, XPS, and Electrochemical Study of Benzenethiol Adsorption on Au(111), *Langmuir*, 1999, **15**, 116–126.

6 S. Ben Amor, G. Baud, M. Jacquet, G. Nansé, P. Fioux and M. Nardin, XPS characterisation of plasma-treated and alumina-coated PMMA, *Applied Surface Science*, 2000, **153**, 172–183.

7 M. Zharnikov, High-resolution X-ray photoelectron spectroscopy in studies of self-assembled organic monolayers, *Journal of Electron Spectroscopy and Related Phenomena*, 2010, **178–179**, 380–393.

8 D. Vaughan, *X-Ray Data Booklet. Center for X-Ray Optics.*, Lawrence Berkeley National Laboratory, 1985.

9 M.-C. Bourg, A. Badia and R. B. Lennox, Gold−Sulfur Bonding in 2D and 3D Self-Assembled Monolayers: XPS Characterization, *J. Phys. Chem. B*, 2000, **104**, 6562–6567.

10 C. Battocchio, F. Porcaro, S. Mukherjee, E. Magnano, S. Nappini, I. Fratoddi, M. Quintiliani, M. V. Russo and G. Polzonetti, Gold Nanoparticles Stabilized with Aromatic Thiols: Interaction at the Molecule–Metal Interface and Ligand Arrangement in the Molecular Shell Investigated by SR-XPS and NEXAFS, *J. Phys. Chem. C*, 2014, **118**, 8159–8168.

11 P. J. Cumpson, The Thickogram: a method for easy film thickness measurement in XPS, *Surf. Interface Anal.*, 2000, **29**, 403–406.

12 H. A. Biebuyck, C. D. Bain and G. M. Whitesides, Comparison of Organic Monolayers on Polycrystalline Gold Spontaneously Assembled from Solutions Containing Dialkyl Disulfides or Alkanethiols, *Langmuir*, 1994, **10**, 1825–1831.

13 K. Yoshihara, The Introduction of Common Data Processing System Version 12, *JSA*, 2017, **23**, 138–148.

14 P. Waske, T. Wächter, A. Terfort and M. Zharnikov, Nitro-Substituted Aromatic Thiolate Self-Assembled Monolayers: Structural Properties and Electron Transfer upon Resonant Excitation of the Tail Group, *J. Phys. Chem. C*, 2014, **118**, 26049–26060.

15 Y. Liu, S. Katzbach, A. Asyuda, S. Das, A. Terfort and M. Zharnikov, Effect of substitution on the charge transport properties of oligophenylenethiolate self-assembled monolayers, *Phys. Chem. Chem. Phys.*, 2022, **24**, 27693–27704.

16 J. Stöhr, *NEXAFS Spectroscopy*, Springer Berlin Heidelberg, Berlin, Heidelberg, 1992, vol. 25.

17 N. Ballav, B. Schüpbach, O. Dethloff, P. Feulner, A. Terfort and M. Zharnikov, Direct Probing Molecular Twist and Tilt in Aromatic Self-Assembled Monolayers, *J. Am. Chem. Soc.*, 2007, **129**, 15416–15417.

18 F. Cecchet, D. Lis, J. Guthmuller, B. Champagne, G. Fonder, Z. Mekhalif, Y. Caudano, A. A. Mani, P. A. Thiry and A. Peremans, Theoretical Calculations and Experimental Measurements of the Vibrational Response of *p* -NTP SAMs: An Orientational Analysis, *J. Phys. Chem. C*, 2010, **114**, 4106–4113.

19 O. Endo, M. Nakamura and K. Amemiya, Depth-dependent C K-NEXAFS spectra for self-assembled monolayers of 4-methylbenzenethiol and 4-ethylbenzenethiol on Au(111), *Journal of Electron Spectroscopy and Related Phenomena*, 2013, **187**, 72–76.